ASSESSMENT OF AEROELASTIC TAILORING EFFECT ON HIGH-ASPECT-RATIO COMPOSITE WING FLUTTER SPEED USING AN OPEN SOURCE REDUCED ORDER MODEL SOLVER

Bertrand Kirsch[1], Olivier Montagnier[1], Emmanuel Bénard,[2], Thierry M. Faure[1]

[1]Centre de Recherche de l'Armée de l'air
École de l'air, BA 701, F-13661 Salon air, France
bertrand.kirsch@defense.gouv.fr · olivier.montagnier@defense.gouv.fr · thierry.faure@defense.gouv.fr
[2]Département Conception et conduite des véhicules Aéronautiques et Saptiaux (DCAS)
Institut Supérieur de l'Aéronautique et de l'Espace - Supaéro
10 avenue Édouard Belin, BP 54032 - 31055 Toulouse CEDEX 4, France
emmanuel.benard@isae.fr

Keywords: fluid/structure interaction, composite materials, aeroelastic tailoring, HAPS

Abstract
The enhancement of high altitude drone endurance compels to design very flexible high-aspect-ratio composite airframe vulnerable to destructive fluid/structure interaction like flutter or torsional divergence. Extensive research has been conducted to increase critical speed without being at the expense of weight balance, one of the promising solutions is the aeroelastic tailoring which consists in a specific configuration of laminated composite layup. The present work presents an aeroelastic reduced order model suitable for the non linear anisotropic behavior of this kind of composite wing implemented in Fortran and Python using optimised open source solver. Along with validation test cases, a simple composite laminate specimen simulation is presented to assess aeroelastic tailoring effect.

1. Introduction

Recent progress made in the field of solar cells, energy storage and composite materials pave the way to a new concept of aircraft, namely High Altitude Pseudo Satellite (HAPS). Among them, a particular type of solar or/and hydrogen powered High Altitude Long Endurance (HALE) Unmanned Aerial Vehicles (UAV) aims to meet a virtually infinite endurance. To achieve this far-reaching goal, because of the low on-board power, aerodynamic and structural performances are stretched to their limits. This results, on the aerodynamic side, in high-aspect ratio wing optimising the lift-to-drag ratio and, on the structural side, in lightweight very flexible composite airframe. The main drawback of this particular design is its vulnerability to destructive fluid/structure interactions like torsional divergence and flutter which are difficult to predict because of the tight coupling between aerodynamics, structure and flight mechanics. Classical solutions designed to further aeroelastic critical speed mostly rely on the stiffening of the airframe or the adjustment of mass distribution. Both options are detrimental to mass balance which is a key feature of HAPS. In that context, alternative solutions should be explored, among these are aeroelastic tailoring which consists in using laminate layup without mirror symmetry or-and unbalanced layup [1]. The emerging structural coupling induced on the aerodynamic side a coupling between the bending due to lift forces and the twisting of the wing which determines the local Angle of Attack (AoA) and consequently a positive impact on aeroelastic behavior.

The computational cost of high fidelity aeroelastic simulation on Very Flexible Aircraft (VFA) is still prohibitive prompting the need for suitable reduced order model. We could mention computation code NANSI (Nonlinear-Aerodynamics/ Nonlinear-Structure Interaction) [2] which combines an Unsteady Vortex Lattice Method (UVLM) and a nonlinear beam theory. The UVLM is particularly useful in case of low-aspect-ratio wing or delta wing because the method is able to predict 3D effects. Another solution is proposed by Murua in SHARP program (Simulation of High Aspect Ratio Planes) [3] using UVLM

with a displacement based geometrically exact beam theory. Some models are dedicated to high-aspect-ratio wing like Drela's program ASWING [4]. This VFA conception tool combines a nonlinear isotropic beam formulation with an unsteady lifting line theory. More recently, Shearer and Cesnik have developed a Matlab toolbox called UM/NAST (University of Michigan/ Nonlinear Aeroelastic Simulation Toolbox) [5] made up of a strain-based geometrically nonlinear beam formulation linked with a finite state two-dimensional incompressible flow aerodynamic theory proposed by Peters et al. [6]. A similar formulation is used by Ribeiro in the Matlab toolbox Aeroflex [7]. Because aeroelastic tailoring exploits the anisotropy of composite materials, a suited reduced order model must take this anisotropy into account. This capability resides in the Matlab toolbox proposed by Patil and Hodges called NATASHA (Nonlinear Aeroelastic Trim and Stability of HALE Aircraft) [8] coupling an intrinsic beam formulation with Peters' theory.

The present paper presents an efficient open source implementation of an aeroelastic reduced order model coupling a nonlinear anisotropic beam theory with unsteady two-dimensional aerodynamic Peters' model. The accuracy of this implementation is then assessed using widely used aeroelastic test cases and then the impact of aeroelastic tailoring is illustrated on a simple laminate specimen.

2. Aeroelastic reduced order model

The high-aspect-ratio assumption gives us the opportunity to neglect three-dimensional effects and thus to use a strip theory which can be easily linked to a beam formulation. A tight coupling is chosen, done by integrating aerodynamic loads directly into the weak formulation of the beam theory. It permits the determination of the aeroelastic modes of the wing about a steady sate, namely frequencies, modal shapes and damping factors. The latter is a key parameter for our study because it defines the limit between stable and unstable speed and thereby provide the flutter boundary.

2.1. Geometrically exact beam theory

In that context, it is essential to ensure a proper modelling of the laminate anisotropy and geometrical non linearity. For this purpose, the choice fell on an open source tool named GEBT (Geometrically Exact Beam Theory) developed by Yu and Blair [9] designed for composite slender structures under large deflections and rotations, assuming the strains to be small. This tool coded in Fortran 90/95 implements a mixed variational formulation based on exact intrinsic equations for dynamics of moving beams developed by Hodges [10]. The exact intrinsic equations for dynamics are derived from Hamilton's weak principle asymptotically developed along the beam axes:

$$\int_{t_1}^{t_2} \int_0^L \left[\delta\left(\boldsymbol{K}-\boldsymbol{U}\right)+\overline{\delta \boldsymbol{W}}\right] dx_1 dt \quad = \quad \overline{\delta \boldsymbol{A}} \tag{1}$$

where t_1 and t_2 are arbitrary fixed times, $\boldsymbol{K}$ and $\boldsymbol{U}$ are the kinetic and strain internal energy, respectively, δ is the usual Lagrangian variation for a fixed time, $\overline{\delta \boldsymbol{W}}$ is the virtual work of applied loads and $\overline{\delta \boldsymbol{A}}$ the virtual action on the same period. The resulting formulation is detailed in Hodges [10].

The main strength of this method compared to classical displacement based formulation is to avoid the dependency from a coordinate system (intrinsic nature) for the position and rotation parameters. Kinematical and constitutive relations are then added to the weak formulation with Lagrange multipliers (mixed nature). The resulting formulation allow a finite element implementation with very simple shape functions (constant or linear). According to Hodges [10], we defined three coordinates systems (figure 1 (a)):

- a unique global body attached frame a $(\vec{x}_a, \vec{y}_a, \vec{z}_a)$ moving with a given linear and angular velocity $\vec{v}_a$ and $\vec{\boldsymbol{\omega}}_a$ in an inertial frame and consistent with flight mechanics conventions ($\vec{x}_a$ pointing upwards, $\vec{y}_a$ pointing the right wing and $\vec{z}_a$ pointing downwards).

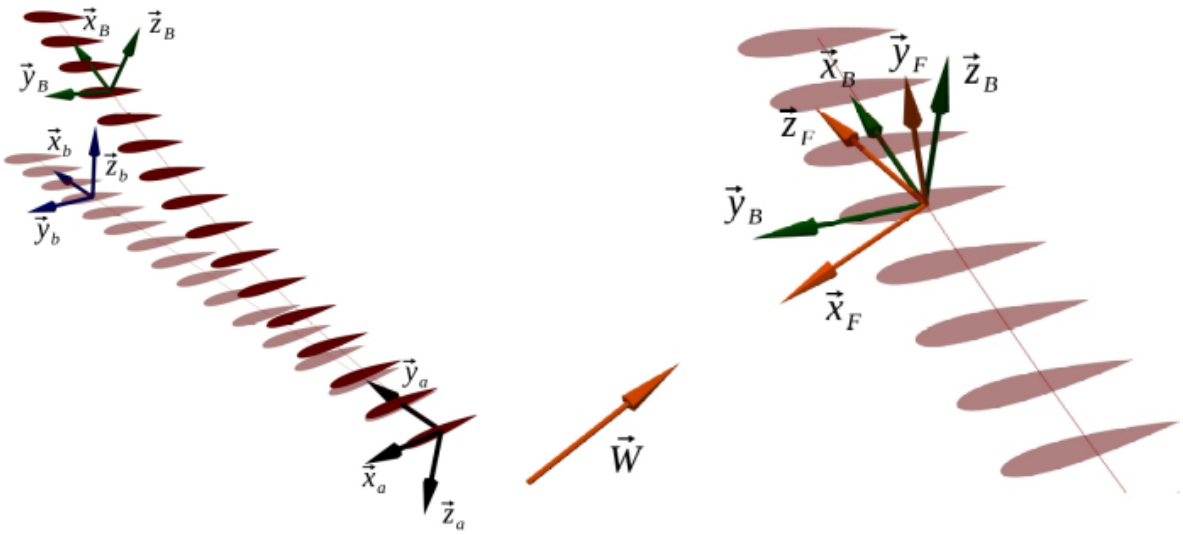

(a) structural frames (b) aerodynamic frame

Figure 1. frames definition

- at least one undeformed beam frame b $(\vec{x}_b, \vec{y}_b, \vec{z}_b)$ fixed in frame a: $\vec{x}_b$ is tangent to the reference line of the undeformed beam. In our case, a frame b is defined for each section of the wing with a different dihedral or/and wing-sweep.
- a deformed beam frame B $(\vec{x}_B, \vec{y}_B, \vec{z}_B)$ for each beam element: $\vec{x}_B$ is tangent to the deformed beam reference line and points to the right, $\vec{y}_B$ has a chordwise direction and points the upstream flow and $\vec{z}_B$ completes the triad.

Fundamentals unknowns of this formulation are the displacement $\vec{u}_a$ and the Rodrigues parameters $\vec{\theta}_a$ in frame a, the internal forces and moments $\vec{F}_B$ and $\vec{M}_B$ in frame B and the linear and angular momenta $\vec{P}_B$ and $\vec{H}_B$ in frame B. The cross section parameters are described by the flexibility matrix and the mass matrix :

$$\begin{Bmatrix} \gamma_{11} \\ 2\gamma_{12} \\ 2\gamma_{13} \\ \kappa_1 \\ \kappa_2 \\ \kappa_3 \end{Bmatrix} = \begin{bmatrix} S_{11} & S_{12} & S_{13} & S_{14} & S_{15} & S_{16} \\ S_{12} & S_{22} & S_{23} & S_{24} & S_{25} & S_{26} \\ S_{13} & S_{23} & S_{33} & S_{34} & S_{35} & S_{36} \\ S_{14} & S_{24} & S_{34} & S_{44} & S_{45} & S_{46} \\ S_{15} & S_{25} & S_{35} & S_{45} & S_{55} & S_{56} \\ S_{16} & S_{26} & S_{36} & S_{46} & S_{56} & S_{66} \end{bmatrix} \begin{Bmatrix} F_1 \\ F_2 \\ F_3 \\ M_1 \\ M_2 \\ M_3 \end{Bmatrix} \tag{2}$$

$$\begin{Bmatrix} P_1 \\ P_2 \\ P_3 \\ H_1 \\ H_2 \\ H_3 \end{Bmatrix} = \begin{bmatrix} \mu & 0 & 0 & 0 & \mu x_{m3} & -\mu x_{m2} \\ 0 & \mu & 0 & -\mu x_{m3} & 0 & 0 \\ 0 & 0 & \mu & \mu x_{m2} & 0 & 0 \\ 0 & -\mu x_{m3} & \mu x_{m2} & i_{22}+i_{33} & 0 & 0 \\ \mu x_{m3} & 0 & 0 & 0 & i_{22} & -i_{23} \\ -\mu x_{m2} & 0 & 0 & 0 & -i_{23} & i_{33} \end{bmatrix} \begin{Bmatrix} V_1 \\ V_2 \\ V_3 \\ \Omega_1 \\ \Omega_2 \\ \Omega_3 \end{Bmatrix} \tag{3}$$

with S_{ij} the coefficients of the flexibility matrix, μ the mass per unit length, x_{m2}, x_{m3} the coordinates of the mass center about respectively $\vec{y}_B$ and $\vec{z}_B$, i_{22} the mass moment of inertia about $\vec{y}_B$, i_{33} the mass moment of inertia about $\vec{z}_B$, i_{23} the product of inertia, $\vec{V}_B$ and $\vec{\Omega}_B$ the linear and angular velocity in the inertial frame developed in frame B, $\vec{\gamma}$ and $\vec{\kappa}$ the strains and curvatures developed in frame B. The anisotropy of the materials is characterised by the non diagonal coefficients of the flexibility matrix. The finite element implementation is detailled in [9] and results in a nonlinear system of $18N + 12$ equations with N the number of beam elements. This formulation is so far purely structural. The aerodynamic part of the reduced order model will thus be injected into it throughout structural distributed forces and moments.

2.2. Cross section homogenisation

In our toolbox, the flexibility matrix can be determined using different methods. In the case of isotropic Euler-Bernoulli beam (shear strains γ_{12} and γ_{13} are neglected, thus line and column 2 and 3 are set to 0), the flexibility matrix (Eq. 2) is greatly simplified:

$$\vec{\vec{S}}^{-1} = \begin{bmatrix} 1/(ES) & 0 & 0 & 0 & 0 & 0 \\ 0 & 0 & 0 & 0 & 0 & 0 \\ 0 & 0 & 0 & 0 & 0 & 0 \\ 0 & 0 & 0 & 1/(GJ) & 0 & 0 \\ 0 & 0 & 0 & 0 & 1/(EI_{G2}) & 0 \\ 0 & 0 & 0 & 0 & 0 & 1/(EI_{G3}) \end{bmatrix} \tag{4}$$

with ES the axial stiffness, GJ the torsional stiffness, EI_{G2} the bending stiffness span-wise and EI_{G3} the bending stiffness chord-wise.

These parameters could be :

- directly derived from test cases data.
- calculated for simple cross section shape (E, G are the Young and Coulomb modulus of the material, S is the cross section area, J is the torsion constant and $I_{G2,3}$ are the second moment of area).

In case of complex cross section shape or anisotropic composite materials, flexibility matrix is determined using an homogenisation tool following a method detailled in [11]. It consists in a three-dimensional finite element calculation realised on a Representative Volume Element (RVE) of the beam using periodic boundary conditions along beam axis direction. The RVE is either a 3D mesh in Abaqus format with a unique element span-wise (airfoil shape for instance) or a laminate plate mesh automatically generated using the preprocessor CalculiX GraphiX. Two dummy nodes are created representing the beam strains and curvatures degrees of freedom (one with γ_{11} and another with κ_1, κ_2 and κ_3). The beam kinematic choice fell on an Euler-Bernoulli hypotheses: shear strain is neglected (line/column 2 and 3 are set to 0), the middle plane of the cross section is normal to the beam axis but warping is nevertheless allowed. This kinematic is imposed using a set of periodic conditions linking strains and curvatures (assimilated to dummy nodes displacements) to the displacements of nodes from opposite faces of the RVE in the beam axis direction described in frame b ($(^-)$ refers to the left face and $(^+)$ to the right face in the sense of increasing beam axis coordinate):

$$u_x^+ - u_x^- = L_x\left(\gamma_{11} + z^+\kappa_2 - y^+\kappa_3\right) \tag{5}$$
$$u_y^+ - u_y^- = L_x\left(-z^+\kappa_1 - \overline{x}\kappa_3\right) \tag{6}$$
$$u_z^+ - u_z^- = L_x\left(y^+\kappa_1 - \overline{x}\kappa_2\right) \tag{7}$$

with $u^+_{x,y,z}$ and $u^-_{x,y,z}$ the nodes displacement of the two periodic faces, L_x the RVE length along beam axis, $\overline{x}$ the coordinate of the middle of the RVE along the beam axis, $y^+$and z^+ are the nodes coordinates within the right face.

Four elementary loading cases are imposed throw the dummy nodes and a linear static calculation is performed using the open source finite element solver CalculiX CrunchiX. For instance, the elementary torsional load case correspond to $M_1 = 1$ and $F_1 = M_2 = M_3 = 0$. Then flexibility matrix forth line or column is identified using the strains and curvatures recorded on the two dummy nodes ($S_{41} = \gamma_{11}$, $S_{44} = \kappa_1$, $S_{45} = \kappa_2$ and $S_{46} = \kappa_3$).

Another implementation of this method could be find for instance in the Abaqus preprocessor *homtools* [12].

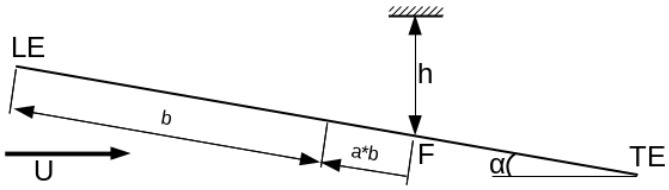

Figure 2. Airfoil parameters

2.3. Finite state induced flow model

Because of the tight coupling between aerodynamic and structure, an unsteady aerodynamic model must be used. To compel with computation needs, a two-dimensional finite state method suited for both time domain and frequency domain simulation is used [6]. This formulation is implemented in our toolbox with the following aerodynamic loads:

$$L = \pi\rho b^2\left(\ddot{h} + U\dot{\alpha} - ba\ddot{\alpha}\right) + 2\pi\rho Ub\left[\dot{h} + U\alpha + b\left(\frac{1}{2} - a\right)\dot{\alpha} - \lambda_0\right] \tag{8}$$

$$M = b\left(\frac{1}{2} + a\right)L - \pi\rho b^3\left[\frac{1}{2}\ddot{h} + u\dot{\alpha} + b\left(\frac{1}{8} - \frac{a}{2}\right)\ddot{\alpha}\right] \tag{9}$$

with L the linear lift, M the linear moment around a reference point F, ρ the air density and U the flow velocity. The semi-chord b, the height h, AoA α and the distance a between the point F and the semi-chord are detailed in figure 2. The induced-flow velocity λ_0 is approximated using N_S induced-flow states $\lambda_1, \lambda_2, \ldots, \lambda_{N_S}$ by:

$$\lambda_0 \approx \frac{1}{2}\sum_{n=1}^{N_S} b_n\lambda_n \tag{10}$$

where the b_n are found in [13] by the least-squares method. The induced-flow dynamics then are derived from the assumption that the shed vorticity stay in the plane of the airfoil and travel downstream with the same velocity as the flow. $\vec{\lambda}$ is a column matrix containing the values of λ_n determined using a set of N_S first-order ODEs (Matrix $\vec{A}$ and vector $\vec{c}$ are defined in [13]):

$$\vec{A}\dot{\vec{\lambda}} + \frac{U}{b}\vec{\lambda} = \left[\ddot{h} + U\dot{\theta} + b\left(\frac{1}{2} - a\right)\ddot{\theta}\right]\vec{c} \tag{11}$$

The aerodynamic model adds N_S equations for each beam element, the coupled aeroelastic system contains $(18 + N_S)\,N + 12$ equations and the same number of unknowns, providing that structural unknowns are completed with $N \times N_S$ induced-flow states λ_{n_i}.

The resulting formulation permits different applications both in time domain and frequency domain. The critical speed computation consists in solving generalised eigenvalue problem and to asses modal damping of the resulting aeroelastic modes. The resolution is made using optimised open source libraries, namely the sparse eigenvalue solver ARPACK and the sparse direct solver MUMPS.

3. Validation test cases

3.1. Isotropic wing

The accuracy of our toolbox is proven using widely used aeroelastic test cases, namely the Goland wing [14] and the Patil wing [15]. The first is universally used among literature and the second is more ap-

Table 1. Goland wing flutter speed and frequency

program	sea level		20000 ft	
	speed (m/s)	frequency (rad/s)	speed (m/s)	frequency (rad/s)
present ($N = 10$; $N_S = 6$)	136.5	70.3	174.9	69.0
Goland [14]	137.2	70.7	-	-
NATASHA[15]	135.6	70.2	-	-
UM/NAST[17]	136.2	70.2	174.9	68.1
SHARP[3]	165	69	-	-
Aeroflex[7]	137.0	70.8	177.0	69.2

Table 2. Patil wing flutter speed and frequency

program	Undeformed wing		Deformed wing	
	speed (m/s)	frequency (rad/s)	speed (m/s)	frequency (rad/s)
present ($N = 10$; $N_S = 6$)	32.2	22.6	23.3	11.9
NATASHA[15]	32.2	22.6	-	-
UM/NAST[18]	32.2	22.6	23.2	10.3
Aeroflex[7]	32.6	22.3	23.4	12.2

propriate to our program because of its high-aspect-ratio. Unfortunately, both of them concern isotropic wing since there is no common anisotropic test case among the literature. Both wing characteristics are detailled in [16]

Results for the Goland wing (Table 1) show a good agreement with other strip theory reduced order models whereas UVLM based models predict a higher critical speed because of three-dimensional effects. A more appropriate test case is the Patil high-aspect-ratio wing. Besides undeformed wing flutter speed assessment, flutter speed is also calculated about the wing deformed by its own weight. Both simulations are made using $N = 10$ and $N_S = 6$ and demonstrate also a good agreement (Table 2).

3.2. Anisotropic laminate specimen

In order to evaluate the impact of aeroelastic tailoring, a simple composite laminate specimen dedicated to wind tunnel test (length:400 *mm*; chord:20 *mm*) is used with different layup. It consists in a 2 *mm* thick Airex C70.75 foam core ($E = 66\ MPa$; $\nu = 0.32$; $\rho = 80\ kg/m^3$) surrounded by two 0.125 *mm* thick carbon fiber T300 plies ($E_l = 181\ GPa$; $E_t = 10.3\ GPa$; $G_{lt} = 7.17\ GPa$; $\nu_{lt} = 0.28$; $\rho = 1600\ kg/m^3$). The layup tested are $[-45/2z_c/\theta]$ with $\theta \in \{-85, 80, ..., 85, 90\}$ and $2z_c = 2\ mm$ the core thickness. Critical speed (flutter and torsional divergence) are then evaluated with regard to structural stiffness (torsional stiffness $1/S_{44}$ and bending stiffness span-wise $1/S_{55}$).

Results are presented on figures 3 and 4 and highlight, on the one hand, the strong effect of upper ply orientation on critical speed, and the absence of a simple relationship between structural stiffness and aeroelastic behavior on the other.

4. Conclusion

Design challenges induced by HAPS in terms of aeroelastic performances show the need for an accurate reduced order model able to simulate nonlinear behavior of an anisotropic high-aspect-ratio wing. The present work presents a solution based of the geometrically exact beam theory coupled with a two-dimensional unsteady finite state aerodynamic model implemented into an open source solver. Accuracy of flutter speed computation on both undeformed and deformed wing has been demonstrated using common aeroelastic test cases. Effect of aeroelastic tailoring, a composite materials technology designed to further flutter speed without being detrimental to mass balance, is then illustrated on a simple laminated sandwich beam with different upper ply orientations. It demonstrates that no simple relationship exists between wing flexibility and flutter speed showing the need for an optimisation process.

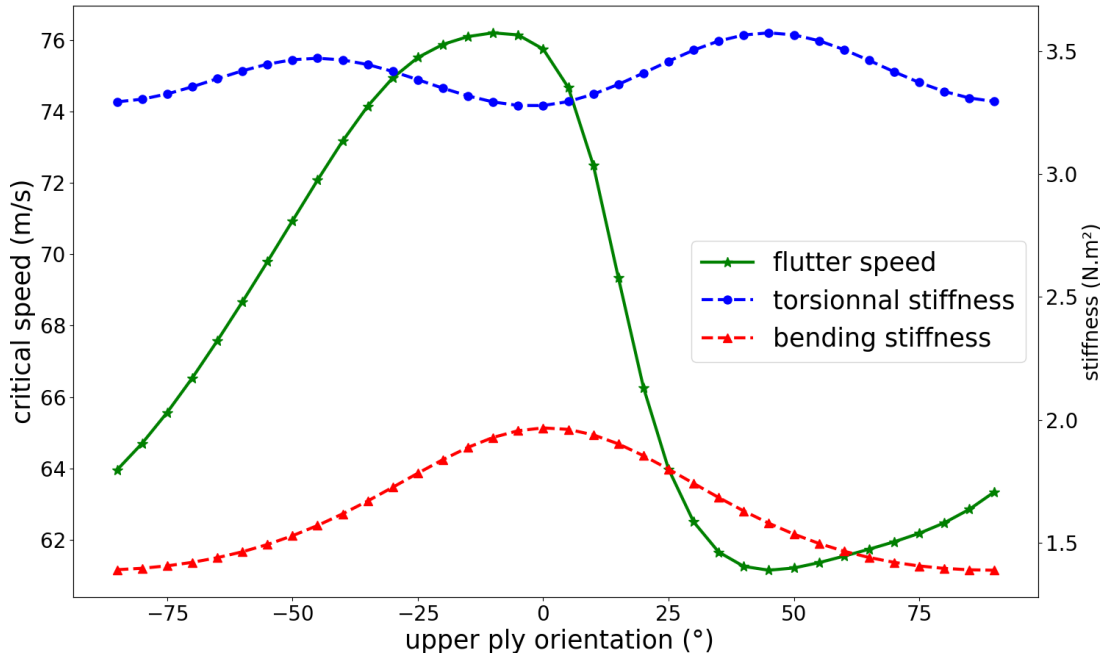

Figure 3. Flutter speed evolution of a wing constitued by a $[-45/2z_c/\theta]$ laminated sandwich beam depending on upper ply orientation θ

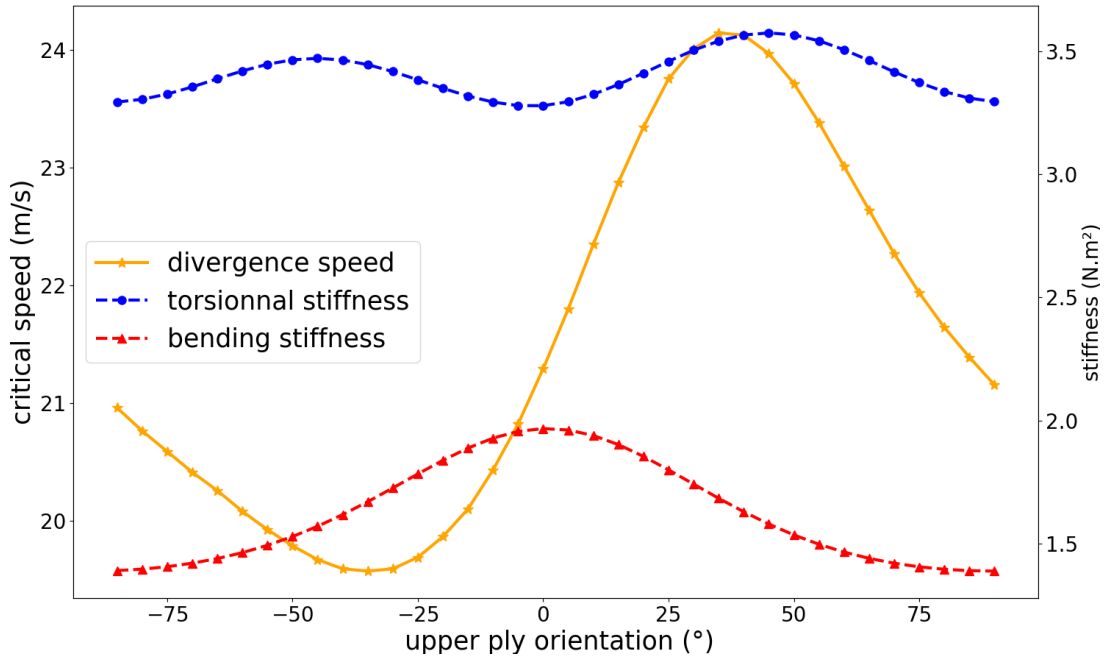

Figure 4. Divergence speed evolution of a wing constitued by a $[-45/2z_c/\theta]$ laminated sandwich beam depending on upper ply orientation θ

References

[1] Bertrand Kirsch, Olivier Montagnier, Emmanuel Bénard et Thierry M. Faure : Dynamic aeroelastic simulation of composite wing for HALE UAV application. *In European Conference for Aeronautics and Space Sciences*, 2017.

[2] Zhicun Wang, P. C. Chen, D. D. Liu et D. T. Mook : Nonlinear-aerodynamics/nonlinear-structure interaction methodology for a high-altitude long-endurance wing. *Journal of Aircraft*, 47(2):556–566, 2010.

[3] Joseba Murua, Rafael Palacios et J. Michael R. Graham : Assessment of wake-tail interference effects on the dynamics of flexible aircraft. *AIAA journal*, 50(7):1575–1585, 2012.

[4] Mark Drela : Integrated simulation model for preliminary aerodynamic, structural, and control-law design of aircraft. *AIAA Paper*, 99:1394, 1999.

[5] Christopher M. Shearer et Carlos ES Cesnik : Nonlinear flight dynamics of very flexible aircraft. *Journal of Aircraft*, 44(5):1528–1545, 2007.

[6] David A. Peters, Swaminathan Karunamoorthy et Wen-Ming Cao : Finite state induced flow models. I-Two-dimensional thin airfoil. *Journal of Aircraft*, 32(2):313–322, 1995.

[7] Flavio Luiz Cardoso Ribeiro, Pedro Paglione, Roberto Gil Annes da Silva et Marcelo Santiago de Sousa : Aeroflex: a toolbox for studying the flight dynamics of highly flexible airplanes. 2012.

[8] C.-S. Chang, Dewey H. Hodges et Mayuresh J. Patil : Flight dynamics of highly flexible aircraft. *Journal of Aircraft*, 45(2):538–545, 2008.

[9] Wenbin Yu et Maxwell Blair : GEBT: A general-purpose nonlinear analysis tool for composite beams. *Composite Structures*, 94(9):2677–2689, 2012.

[10] Dewey H. Hodges : A mixed variational formulation based on exact intrinsic equations for dynamics of moving beams. *International journal of solids and structures*, 26(11):1253–1273, 1990.

[11] Patrice Cartraud et Tanguy Messager : Computational homogenization of periodic beam-like structures. *International Journal of Solids and Structures*, 43(3-4):686–696, 2006.

[12] HOMTOOLS - Homogeneization toolbox for Abaqus - http://homtools.lma.cnrs-mrs.fr/.

[13] Dewey H. Hodges et G. Alvin Pierce : *Introduction to structural dynamics and aeroelasticity*, volume 15. cambridge university press, 2011.

[14] Martin Goland et Y. L. Luke : The flutter of a uniform wing with tip weights. *Journal of Applied Mechanics*, 15(1):13–20, 1948.

[15] Mayuresh J. Patil : *Nonlinear aeroelastic analysis, flight dynamics, and control of a complete aircraft*. Thèse de doctorat, Citeseer, 1999.

[16] Bertrand Kirsch, Olivier Montagnier, Emmanuel Bénard et Thierry M. Faure : Computation of very flexible high-aspect-ratio composite wing flutter speed using optimised open source solver. *In 53rd 3AF International Conference on Applied Aerodynamics Multiphysics approach in Aerodynamics*, Salon de Provence, France, mars 2018.

[17] Eric Lee Brown : *Integrated strain actuation in aircraft with highly flexible composite wings*. Thèse de doctorat, Massachusetts Institute of Technology, 2003.

[18] Weihua Su : *Coupled nonlinear aeroelasticity and flight dynamics of fully flexible aircraft*. Thèse de doctorat, University of Michigan, 2008.